RSC Advances

Volume 1 | Number 1 | Jan 2013 | Pages 1–100

RSC Advances

www.rsc.org/advances

ROYAL SOCIETY OF CHEMISTRY

www.rsc.org/advances

Table of contents

N-doped arch and hollow nano-carbons exhibit 4.23 mmol g^{-1} CO_2 adsorption; ~13% CO_2/N_2 selectivity; and 98% regenerative capability at ambient conditions.

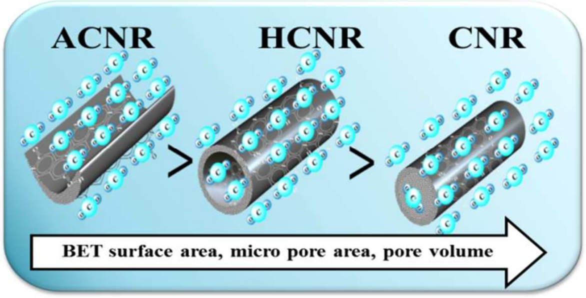

RSC ADVANCES

RSCPublishing

COMMUNICATION

Cite this: DOI: 10.1039/x0xx00000x

Nitrogen-doped arch and hollow shaped nanocarbons for CO_2 adsorption

Prakash Ramakrishnan, Sangaraju Shanmugam

Received 00th August 2014,
Accepted 00th August 2014

DOI: 10.1039/x0xx00000x

www.rsc.org/

We report arch and hollow nanocarbons with high nitrogen content and appreciable surface area are highly capable to CO_2 adsorption (4.23 mmol g^{-1}), selectivity (CO_2/N_2: ~13%) and facile regeneration (98%) at ambient conditions, respectively.

An inefficient CO_2 sequestration during post- and pre-combustion process from the energy sectors venting of CO_2 to atmosphere and increase it concentration in the atmosphere which directly impact on global warming, a serious concern for our civilization.[1] The conventional state-of-the-art CO_2 sorbent (alkanolamine solution) using in the power plant having critical issues on corrosion control and additional energy consumption for sorbent regeneration.[2] Alternatively, various promising porous sorbents such as metal-organic frameworks (MOFs), microporous zeolites and activated carbons have been reported.[3–5] Owing to the stringent industrial requirements majority of MOFs and Zeolites could be restricted in practical usage, due to the complex and expensive synthesis approach, despite of having their best CO_2 sorbent characteristics. So, the development of an alternate porous sorbent is needed with good CO_2 selective adsorption and regeneration for industrial realization are still a major task.

In recent decades, porous carbon materials a class of nanocarbons find potential applications in energy storage, gas adsorption, molecular separation, catalysis, and so on due to their tunable structural texture, impoundable surface functionality, chemical stability, low price and easy availability in versatile forms such as fibers, powders, sheets, foams, composites and tubes, etc.[6–10] Porous carbon with surface functionalized groups having high surface area are mostly desirable for obtaining high electro-sorption and gas sorption properties.[11] Nitrogen functionalized carbon materials have drawn much attention in CO_2 adsorption as N-doping generate the basic groups to promote the absorption of acidic CO_2 gas.[12] Mostly, N-doped porous carbons are prepared by two common approaches; post heat treatment synthesis using high surface area carbon materials under N-source and in-situ synthesis approach, i.e., hard and soft template approach.[13–16] However, in the former approach low N-content results and in the latter approach complicated microphase separation, need of expensive templates for synthesis, toxic chemicals for etching and time consuming tedious carbonization process results.[17] Alternatively, using electrospinning high N-content can be obtained using N-source polymers.[18] However, the N-doped carbon material results in this approach often deliver limited surface area due to the cylindrical fiberous morphology. Thus, post activation process using KOH treatment (physical or chemical activation) was adopted to increase the surface area, but with the cost of high N-content.[19] Thus, a method to fabricate N-doped nanocarbon with high surface area using facile and cost-effective for CO_2 adsorption is also necessary to utilize in CO_2 capture applications.

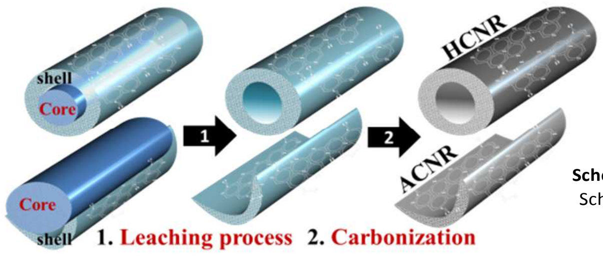

Scheme 1. Schematic representation of HCNR and ACNR synthesis steps.

---

* Department of Energy Systems Engineering, Daegu Gyeongbuk Institute of Science & Technology (DGIST), 50-1 Sang-Ri, Hyeongpung-Myeon, Dalseong-gun, Daegu, 711-873, Republic of Korea.
Tel.: +82-53-785-6413. Fax: +82-53-785-6409.
E-Mail address: sangarajus@dgist.ac.kr

† Electronic Supplementary Information (ESI) available: Figures of FE-SEM, FE-TEM, N_2 adsorption-desorption, Tables of deconvoluted XPS analysis for all samples. See DOI: xx.xxxx/x000000x/

Herein, we meticulously designed a new class of carbon material with a high level N-doping and appreciable surface area. The porous carbon nanostructures with different morphologies were fabricated via a co-axial electrospinning approach, followed by leaching of sacrificial material using hot de-ionized water and a subsequent carbonization under inert atmosphere. Thus, two different N-doped carbon nanostructures, hollow (HCNR) and arch (ACNR) shaped morphologies were obtained. The developed N-doped ACNR materials exhibit a high textural properties along with a high N-content under an ambient conditions, 298 K and 1 bar, in CO_2 capture studies a maximum CO_2 adsorption of 4.23 mmol g^{-1}, good CO_2 selectivity of ~13, and regenerable capable of 98%, was obtained.

The fabricated N-doped porous HCNR and ACNR is illustrated in Scheme 1. The co-axially prepared electro-spun fibrous membrane of HCNR and ACNR samples display the average diameter of 270 and 330 nm, respectively. During leaching process, the hydrophilic PVP core material was leached out completely from electro-spun HCNR and ACNR membranes. Finally, carbonization of HCNR material displays a hollow structure with a core diameter of 40 to 70 nm; carbonized ACNR material displays the arch-shaped nanostructure or semi hollow carbon nanostructures. Further, diameter of HCNR and ACNR decreases to 180 and 155nm, respectively (Fig. 1b, d).

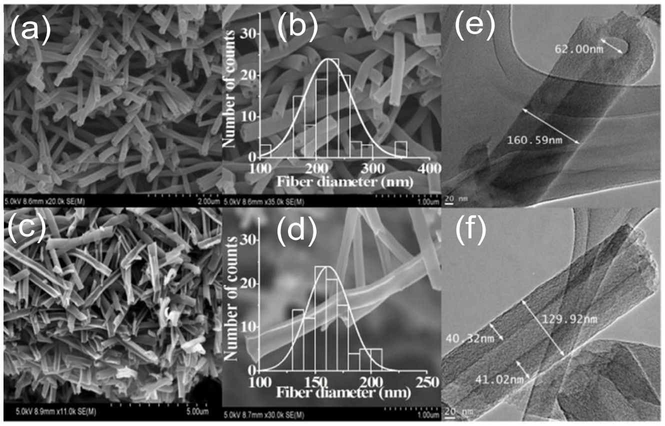

Fig. 1 HCNR sample FE-SEM (a, b) and FE-TEM (e) images; ACNR sample FE-SEM (c, d) and FE-TEM (f) images.

Further, FE-TEM image in Fig. 1(e, f) confirms the morphologies of HCNR and ACNR samples. For comparison, carbon nanorods (CNR) was fabricated using a single spinneret electrospinning approach and carbonized using same parameters was followed in ACNR and HCNR samples; the carbonized CNR displays a typical cylindrical rod shaped morphology as shown in Fig. S1 a-d.

The XRD spectra reveals that all the carbonized samples were turbostatic carbon in nature (Fig. S2). Through CHNS elemental analysis the N- content was found at 8.51, 7.53 and 8.07 weight % for CNR, HCNR and ACNR samples, respectively. The XPS of N-doped carbon nanostructures show strong signals of carbon, nitrogen and oxygen. The deconvoluted N 1s spectra of all samples show existence of pyridinic-N and quaternary-N (Fig. S3). It is noted that the nitrogen functionalities act as a Lewis base sites, which are active for CO_2 sequestration.[20] The peak deconvolution analysis shows the amount of pyridinic (N1) in CNR, HCNR and ACNR sample were found to be 30, 37 and 35%, respectively.

A Bruner–Emmett–Teller (BET) measurement (Fig. S4 and Table S2) reveals that ACNR, HCNR and CNR samples exhibit BET surface area (S_{BET}) of 619, 557 and 484 m2 g^{-1}, respectively. The t-plot micropore surface areas for ACNR, HCNR and CNR are 432, 417 and 334 m^2 g^{-1}, indicating 70-74% microporosity in all the samples (Table S2). The total pore volume from NL-DFT studies for ACNR, HCNR and CNR samples are 0.6589, 0.5681 and 0.4803 cm^3 g^{-1}, respectively. The ACNR and HCNR samples exhibit high surface area, pore volume and micro-pore area which could be highly suitable for gas sorption applications such as H_2, CH_4, CO_2 capture application.

To counter a major greenhouse gas component, CO_2, our N-doped porous carbon materials for CO_2 sequestration performance were employed. Fig. 2a shows the CO_2 and N_2 adsorption isotherms of ACNR, HCNR and CNR at 298 K, which shows a maximum CO_2 adsorption of 4.23 mmol g^{-1} at 1 bar was observed for ACNR than the other materials. Also, at 273K ACNR exhibits a high adsorption of 6.53 mmol g^{-1} at 1 bar (Fig. S5a and Table. 1). Such high CO_2 adsorption of ACNR is due to a high surface area (619 m^2 g^{-1}), a high pore volume (0.6589 cm^3 g^{-1}) and a high N-content (8.70 wt%). Also, the N-species from pyridinic group, as explained in XPS studies, existence in all N-doped carbon nanostructures act as a Lewis base site for CO_2 adsorptions, particularly in a low pressure region plays a vital role.[20] In addition, ACNR and HCNR samples display no saturation limit of CO_2 at 1 bar in comparison to CNR, which indicate that high CO_2 adsorption could be possible at elevated pressure. The same phenomenon of CO_2 capture was even observed at various temperature 273 K, 293 K and 303 K (Fig. S5a-c) and the obtained results are listed in the Table 1. In comparison, cylindrical CNR sample shows a poor CO_2 adsorption because of its low surface area, despite of having high N-content.

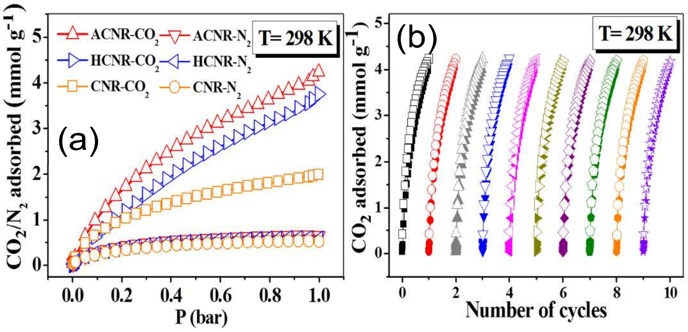

Fig. 2 (a) CO_2 adsorption and CO_2/N_2 selectivity test formed at 298K for all samples, (b) CO_2 regenerative test for ACNR at 298 K using high purity CO_2 gas.

The comparison of CO_2 capture of various N-doped- and N-free state-of-the-art of carbon sorbents suggest that higher and comparable CO_2 adsorption capacities for ACNR and HCNR samples was achieved (Table S3). It is clear from the comparison that N-doped ACNR could be considered amongst the potential N-doped carbon materials for CO_2 adsorption application.

In addition to CO_2 adsorption evaluation, the selectivity of flue gas components, predominately N_2 gas (70-70 %), is crucial for power plants during the post combustion process. It is also to be expected the presence of N-content could preferentially adsorb CO_2 over N_2.[21] Thus the ideal adsorption solution theory (IAST) was used to evaluate selectivity of CO_2/N_2 for all samples. As shown in Fig. 2a, the selectivity of CO_2 over N_2 gas at 298 K for ACNR, HCNR and CNR was found as 13.53, 9.63, and 8.87, respectively, which reveals that ACNR sorbent has potentially endurance towards CO_2 gas. Also, ACNR selectivity is higher than other porous materials, such as MOF-253 possesses selectivity of 12.[22]

For industrial CO_2 capture application, the adsorbent should possess the critical criteria of high cyclic stability towards CO_2. To ascertain, the CO_2 regenerative/cycle test for the best CO_2 adsorption sample, ACNR, tested for ten consequent adsorption-desorption processes at 298 K, vacuum evacuation was provided at each cycle, (Fig. 2b) which revealed that ACNR has 98% CO_2 retention after 10 cycles. Thus, an ACNR sample with high CO_2 adsorption, good selectivity and regenerative capability characteristics were impressive for industrial applications.

Table 1. CO_2 adsorption/separation performances of N-doped ACNR, HCNR and CNR samples.

Sample	CO_2 capture at 1 bar in				CO_2/N_2 selectivity at 298 K		CO_2/N_2*
	273K	293K	298K	303K	At 0.15 bar	At 0.85 bar	
ACNR	6.53	4.49	4.23	3.95	1.51	0.63	13.53
HCNR	6.00	4.16	3.75	3.58	1.00	0.59	9.63
CNR	2.72	2.58	1.98	1.75	0.84	0.51	8.87

*From IAST at CO_2:N_2 ratio of 0.15: 0.85 bar at 298 K.

Also, to determine the strength of interaction between CO_2 and our N-doped carbon materials the isosteric heat of adsorption (Q_{st}) was calculated using the Clausius-Clapeyron equation for CO_2 isotherms performed at 273, 293, 298 and 303 K (Fig. S5 d). The Q_{st} evaluated for all samples indicates the physisorption nature of an absorbent i.e, weak Vander Waals forces. Also, it can be found that N-content in all the samples could substantially improve the isosteric heat of adsorption at low coverage, but the micropores play vital role in high coverage which overshadows the N-content role. From the observation, ACNR had the highest Q_{st} value 36.27 kJ mol^{-1}; HCNR and CNR have lowest Q_{st} value of 20.80 kJ mol^{-1} and CNR 7.8 kJ mol^{-1}, respectively. In general, a high Q_{st} is a necessary criteria for flue gas separation, owing to a high CO_2 uptake at very low pressure. At the same time too high Q_{st} which result chemisorption would cause difficulty in the regeneration of sorbents.[23] Notably, ACNR having Q_{st} of 36.27 kJ mol^{-1} are highly suitable for flue gas separations.

In summary, we have successfully developed high N-content and surface area of N-doped nano carbons, using a simple co-axial electrospinning technique. Their CO_2 uptake properties were demonstrated as superior in all aspects such as higher CO_2 uptake amounts, selectivities for CO_2 at low pressure, regenerative capability and much higher isosteric heat of adsorptions. Such cost effective and appreciable CO_2 sequestration nanocarbons could possibly meet the commercial CO_2 sorbents criteria. Further, we hope that this unique N-doped nanocarbon structures would open new opportunities in applications related to H_2 adsorption, electro-catalyst for CO_2 reduction, energy storage, separation, and medicine.

This work was supported by the DGIST R&D Program of the Ministry of Education, Science and Technology of Korea (14-BD-01) and also partly by the DGIST MIREBraiN program.

Notes and references

1. S. Yeh, S. M. Jordaan, A. R. Brandt, M. R. Turetsky, S. Spatari, and D. W. Keith, *Environ. Sci. Technol.*, 2010, **44**, 8766–72.
2. D. M. D'Alessandro, B. Smit, and J. R. Long, *Angew. Chem. Int. Ed. Engl.*, 2010, **49**, 6058–82.
3. J. An, R. P. Fiorella, S. J. Geib, and N. L. Rosi, *J. Am. Chem. Soc.*, 2009, **131**, 8401–3.
4. O. M. Yaghi, M. O'Keeffe, N. W. Ockwig, H. K. Chae, M. Eddaoudi, and J. Kim, *Nature*, 2003, **423**, 705–14.
5. O. K. Farha, a Ö. Yazaydın, I. Eryazici, C. D. Malliakas, B. G. Hauser, M. G. Kanatzidis, S. T. Nguyen, R. Q. Snurr, and J. T. Hupp, *Nat. Chem.*, 2010, **2**, 944–8.
6. Y. Gogotsi, A. Nikitin, H. Ye, W. Zhou, J. E. Fischer, B. Yi, H. C. Foley, and M. W. Barsoum, *Nat. Mater.*, 2003, **2**, 591–4.
7. Z.-S. Wu, Y. Sun, Y.-Z. Tan, S. Yang, X. Feng, and K. Müllen, *J. Am. Chem. Soc.*, 2012, **134**, 19532–5.
8. R. K. Motkuri, H. V. R. Annapureddy, M. Vijaykumar, H. T. Schaef, P. F. Martin, B. P. McGrail, L. X. Dang, R. Krishna, and P. K. Thallapally, *Nat. Commun.*, 2014, **5**, 4368.
9. H. Wang, Q. Gao, and J. Hu, *J. Am. Chem. Soc.*, 2009, **131**, 7016–22.
10. J. Wang, H. Zhong, Y. Qin, and X. Zhang, *Angew. Chem. Int. Ed. Engl.*, 2013, **52**, 5248–53.
11. Y. Li, T. Ben, B. Zhang, Y. Fu, and S. Qiu, *Sci. Rep.*, 2013, **3**, 2420.
12. C.-C. Hwang, J. J. Tour, C. Kittrell, L. Espinal, L. B. Alemany, and J. M. Tour, *Nat. Commun.*, 2014, **5**, 3961.
13. D. Hulicova-Jurcakova, M. Seredych, G. Q. Lu, and T. J. Bandosz, *Adv. Funct. Mater.*, 2009, **19**, 438–447.
14. D. Guo, J. Mi, G. Hao, W. Dong, G. Xiong, W. Li, and A.-H. Lu, *Energy Environ. Sci.*, 2013, **6**, 652-9.
15. D. Hulicova, M. Kodama, and H. Hatori, *Chem. Mater.*, 2006, **18**, 2318–2326.
16. C. Liang, Z. Li, and S. Dai, *Angew. Chem. Int. Ed. Engl.*, 2008, **47**, 3696–717.
17. L. Hao, X. Li, and L. Zhi, *Adv. Mater.*, 2013, **25**, 3899–904.
18. S. Cavaliere, S. Subianto, I. Savych, D. J. Jones, and J. Rozière, *Energy Environ. Sci.*, 2011, **4**, 4761-85.
19. A. Greiner and J. H. Wendorff, *Angew. Chem. Int. Ed. Engl.*, 2007, **46**, 5670–703.
20. H. Chen, F. Sun, J. Wang, W. Li, W. Qiao, L. Ling, and D. Long, *J. Phys. Chem. C*, 2013, **117**, 8318–28.

21. D. M. D'Alessandro, B. Smit, and J. R. Long, *Angew. Chem. Int. Ed. Engl.*, 2010, **49**, 6058–82.
22. E. D. Bloch, D. Britt, C. Lee, C. J. Doonan, F. J. Uribe-Romo, H. Furukawa, J. R. Long, and O. M. Yaghi, *J. Am. Chem. Soc.*, 2010, **132**, 14382–4.
23. Y. Zhao, X. Liu, K. X. Yao, L. Zhao, and Y. Han, *Chem. Mater.*, 2012, **24**, 4725–34.